Volume 9
Number 36
28 September 2021
Pages 7281–7568

Journal of Materials Chemistry B

Materials for biology and medicine

rsc.li/materials-b

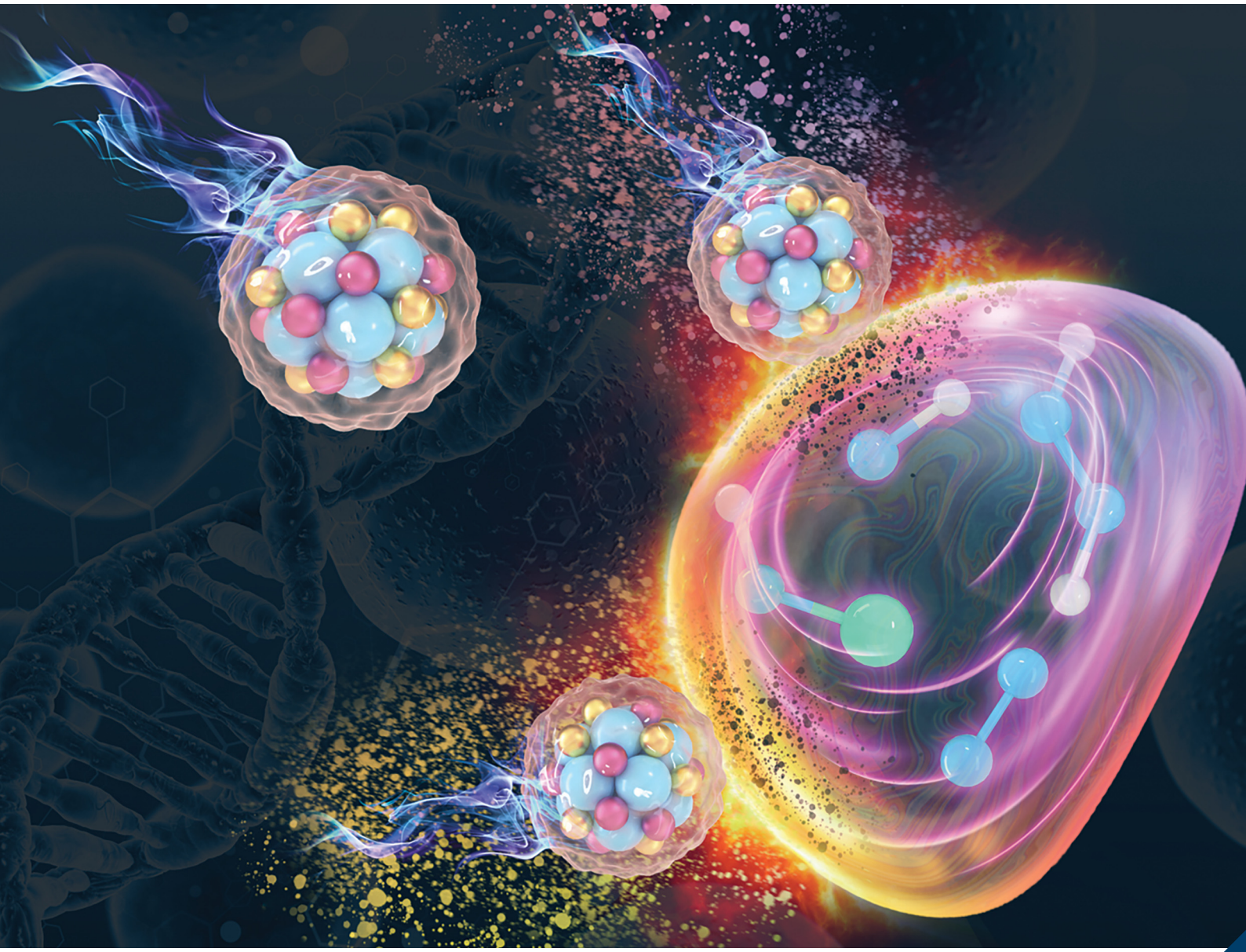

ISSN 2050-750X

ROYAL SOCIETY OF CHEMISTRY

REVIEW ARTICLE

Yuao Wu and Hang T. Ta

Different approaches to synthesising cerium oxide nanoparticles and their corresponding physical characteristics, and ROS scavenging and anti-inflammatory capabilities

Indexed in Medline!

Journal of Materials Chemistry B

ROYAL SOCIETY OF CHEMISTRY

REVIEW

Cite this: *J. Mater. Chem. B*, 2021, **9**, 7291

Different approaches to synthesising cerium oxide nanoparticles and their corresponding physical characteristics, and ROS scavenging and anti-inflammatory capabilities

Yuao Wu[a] and Hang T. Ta *[abc]

Received 14th May 2021,
Accepted 10th July 2021

DOI: 10.1039/d1tb01091c

rsc.li/materials-b

The biological applications of cerium oxide nanoparticles (nanoceria) have received extensive attention in recent decades. The coexistence of trivalent cerium and tetravalent cerium on the surface of nanoceria allows the scavenging of reactive oxygen species (ROS). The regeneratable changes between Ce^{3+} and Ce^{4+} make nanoceria a suitable therapeutic agent for treating ROS-related diseases and inflammatory diseases. The size, morphology and Ce^{3+}/Ce^{4+} state of cerium oxide nanoparticles are affected by the synthesis method. This review focuses on various synthesis methods of cerium oxide nanoparticles and discusses their corresponding physical characteristics, and anti-ROS and anti-inflammatory properties.

1 Introduction

Cerium is a lanthanide element and a rare earth metal. Its oxides can be CeO_2 and Ce_2O_3 as cerium can be either trivalent (Ce^{3+}) or tetravalent (Ce^{4+}).[1] Cerium oxide is widely used as a polishing agent,[2] catalyst,[3] preservative,[4] and sensor[5] in industry. With the development of nanotechnology,[6,7] biomedical applications of cerium oxide nanoparticles have been increasingly reported.[8,9] Studies showed that nanoceria could be used as superoxide dismutase (SOD) mimetics,[10] catalase (CAT) mimetics,[11] scavengers of nitric oxide radicals[12] and hydroxyl radicals.[13]

Since the concept of reactive oxygen species (ROS) was proposed in 1947, research on active oxidants and antioxidants has not been interrupted.[14] Excess ROS has emerged as a critical factor in many chronic diseases, such as atherosclerosis,[15] rheumatoid arthritis,[16] hepatitis[17] and other inflammatory diseases.[18] Recently, the anti-ROS and anti-inflammatory properties of cerium oxide nanoparticles have been investigated and confirmed by several studies.[19–21] A number of novel synthesis methods of cerium oxide nanomaterials have also been reported.[22] The characteristics and functions of cerium oxide nanomaterials were shown to be related to their synthesis methods.

Cerium oxide nanoparticles are unique due to their convertible surface. Both trivalent cerium atoms (Ce^{3+}) and tetravalent cerium atoms (Ce^{4+}) are on the surface of cerium oxide.[23] Ce^{3+} on the surface works as an analogue of superoxide dismutase. It can transform superoxide radicals into oxygen and hydrogen peroxide ($Ce^{3+} + O_2^{-\bullet} + 2H^+ \rightarrow Ce^{4+} + H_2O_2$). It was also reported that Ce^{3+} could reduce H_2O_2 to H_2O ($2Ce^{3+} + H_2O_2 + 2H^+ \rightarrow 2Ce^{4+} + 2H_2O$). Ce^{4+} produced by the above-mentioned reactions can also scavenge hydrogen peroxide and generate oxygen and water, eventually eliminating ROS. Due to the absorption of hydrogen electrons, Ce^{4+} is then converted into the original Ce^{3+} ($2Ce^{4+} + H_2O_2 + 2OH^- \rightarrow 2Ce^{3+} + O_2 + 2H_2O$)[10] (Fig. 1A). Hence, this irreplaceable anti-ROS property allows cerium oxide to be utilised as a potential regenerative ROS scavenger.[24–29]

There are few reviews that discuss the synthesis[30,31] and biomedical applications[32,33] of cerium oxide nanoparticles. However, as research interest in the anti-ROS and anti-inflammatory properties of nanoceria increases, a review with a detailed discussion on their synthesis methods, surface valence states, and anti-ROS and anti-inflammatory properties is urgently needed. Our review fills this gap. In this review, typical synthesis methods and also novel green synthesis methods of cerium oxide nanoparticles are comprehensively discussed (Fig. 1B). The size, morphology and Ce^{3+}/Ce^{4+} state of cerium oxide nanoparticles are compared between different synthesis methods. Then, the anti-ROS and anti-inflammatory abilities of cerium oxide nanoparticles are reviewed. Lastly, the future expectation of cerium oxide nanoparticles is discussed.

2 Synthesis of cerium oxide nanoparticles

Various methods of synthesising cerium oxide nanoparticles have been reported in the last few decades. Studies indicated that

[a] *Queensland Micro- and Nanotechnology, Griffith University, Nathan, Queensland 4111, Australia. E-mail: h.ta@griffith.edu.au*
[b] *School of Environment and Science, Griffith University, Nathan, Queensland 4111, Australia*
[c] *Australian Institute for Bioengineering and Nanotechnology, The University of Queensland, St Lucia, Queensland 4072, Australia*

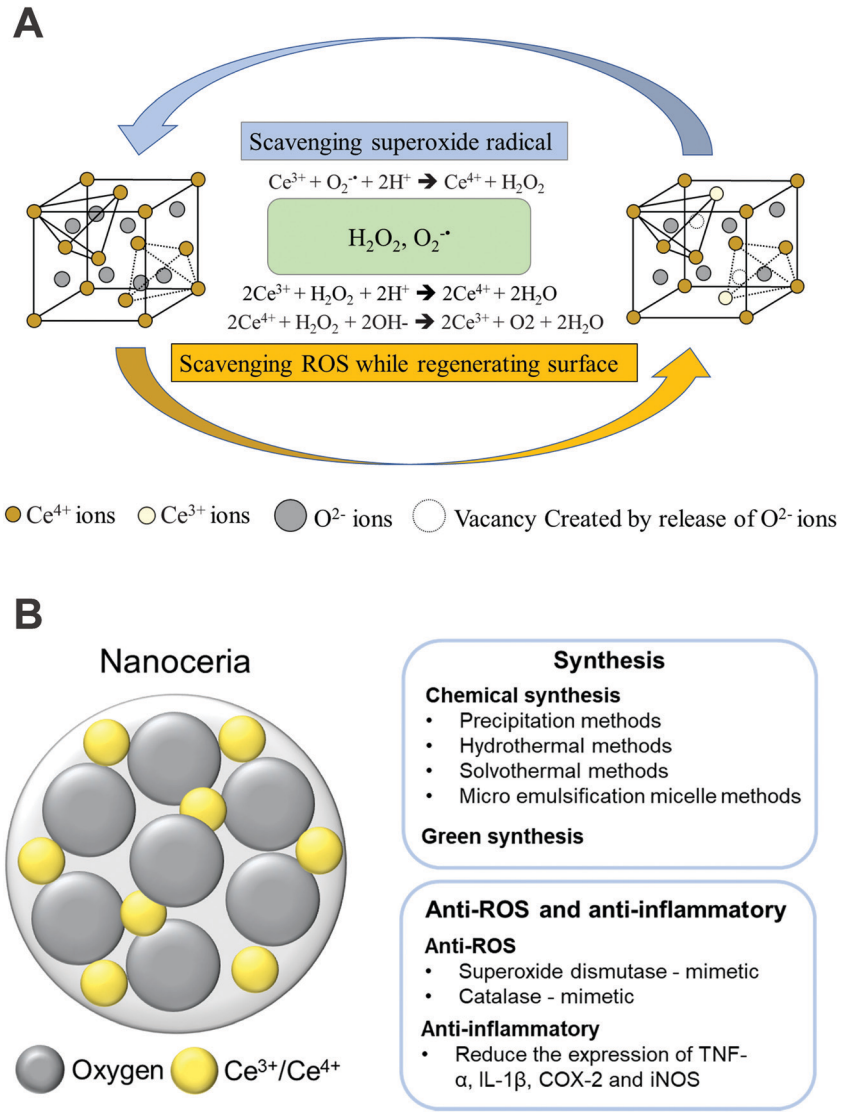

Fig. 1 Overview of cerium oxide nanoparticles. (A) Regenerative antioxidant properties of cerium oxide nanoparticles. (B) Synthesis, and anti-ROS and anti-inflammatory properties of cerium oxide nanoparticles.

different synthesis methods could affect the size, morphology and surface valence of cerium oxide nanoparticles. Conventional chemical synthesis is the major approach to synthesising nanoceria. Recently, novel bio-directed synthesis methods (green synthesis) have also been reported.

2.1 Conventional chemical synthesis

A number of chemical synthesis methods of cerium oxide nanoparticles were described, including precipitation,[34–36] hydrothermal,[37–39] solvothermal,[40] sol–gel[41] and microemulsification micelle methods.[42]

Table 1 Synthesis of cerium oxide nanoparticles using precipitation methods

Precursors		Reactant		Size (nm)	Surfactant/coating	Morphology	Valence states	Ref.
Cerium(III) nitrate hexahydrate (mol L^{-1})	0.4	Ammonium hydroxide (mol L^{-1})	0.4	13–33	Citrate acid/EDTA	Nanosphere	Ce^{3+} & Ce^{4+}	43
Cerium(III) nitrate hexahydrate (mol L^{-1})	0.2	Ammonium hydroxide (mol L^{-1})	2.3	12	N/A	Nanohexagon	Ce^{3+} & Ce^{4+}	44
	0.2		2.3	6	Monosodium phosphate	Nanosphere		
	0.2		2.3	7	Sodium bisulfate	Nanosphere		
Ammonium cerium(IV) nitrate	0.2		2.3	2.6	N/A	Nanohexagon		
	0.2		2.3	2.7	Monosodium phosphate	Nanosphere		
	0.2		2.3	2.6	Sodium bisulfate	Nanosphere		
Ammonium cerium(IV) nitrate	0.11	Ammonium hydroxide (mol L^{-1})	9.8	6	Poly(acrylic acid)	Nanosphere	Ce^{3+} : Ce^{4+} 1.28 : 1	45

2.1.1 Precipitation methods. Table 1 summarises the precipitation methods used for the synthesis of cerium oxide nanoparticles. In the precipitation reaction, nanoceria are obtained by adding reactant ligands (such as sodium hydroxide or ammonium hydroxide) to the metal ion solution (precursors). Cerium(III) nitrate hexahydrate is one of the most used precursors. In a study by Lin *et al.*,[43] the effect of reactant ligands was reported. Sodium hydroxide or ammonium hydroxide was reacted with cerium(III) nitrate hexahydrate separately. The results suggested that the nanoceria synthesised by ammonium hydroxide had a smaller size compared to the ones synthesised by sodium hydroxide. Ammonium-involved nanoceria also had better stability and regular spherical shape. Large agglomeration of particles was observed in sodium hydroxide-derived nanoceria. In another study where the precipitation method was applied, Yurova *et al.*[44] sought to investigate the effect of precursors and acidic modification on cerium oxide nanoparticles. In the reaction, ammonium cerium(IV) nitrate and cerium(III) nitrate hexahydrate were used as two different sources of nanoceria. Transmission electron microscopy (TEM) images showed that cerium(III)-derived nanoceria have a bigger size (6–12 nm) than cerium(IV)-derived nanoceria (2–3 nm). The morphology of nanoparticles could be changed from hexagons to spherical or ellipsoidal when the particles were treated with sulphate acid and phosphate acid. In addition, poly(acrylic acid) has been reported to be the common coating of the cerium oxide nanoparticles. The resulting nanoparticles were synthesised by ammonium cerium(IV) nitrate and ammonium hydroxide and had a hydrodynamic diameter of 6 nm and both Ce^{3+} and Ce^{4+} on the surface.[45]

2.1.2 Hydrothermal methods. Table 2 summarises the hydrothermal methods used to synthesise cerium oxide nanoparticles. The main differences between precipitation and hydrothermal methods are temperatures and pressures. Trenque *et al.*[37] suggested that the morphology of the resulting nanoceria could be manipulated by different parameters in hydrothermal methods (Fig. 2a). Under the same reactant concentration of cerium(III) nitrate hexahydrate and sodium hydroxide, cerium oxide nanorods could be synthesised in 6 hours by heating at 100 °C, while cerium oxide nanocubes were produced in 24 hours by incubating at 180 °C in a Teflon-lined stainless steel autoclave. When replacing sodium hydroxide with ammonium hydroxide, truncated octahedra and polyhedral nanoceria have been observed under a TEM. Besides, the morphology of cerium oxide could also change from truncated octahedra to octahedra by reducing the concentration of ammonium hydroxide. Another study indicated that polyhedral nanoceria have a higher Ce^{3+} ratio (25.3%) on the surfaces than cerium oxide nanorods (24.3%) and cerium oxide nanocubes (23.3%) (Fig. 2b).[47] In a study by Liu and coworkers,[48] cerium oxide nanocubes with a size of 5 nm were synthesised from ammonium cerium(IV) nitrate and acetic acid. Cerium oxide nanocubes (100% of Ce^{4+} on the surface) were successfully encapsulated inside the reductive apoferritin (AFt–CeO_2), which increased the percentage of Ce^{3+} on the surface of cerium oxide nanoparticles from 0% to 70%. They also investigated the ROS scavenging ability of these nanoceria. The results indicated that AFt–CeO_2 had a better ROS scavenging efficiency (70%) than cerium oxide nanocubes (20%) in H_2O_2-treated HepG2 cells.

2.1.3 Solvothermal methods. Table 3 summarises the solvothermal methods used to synthesise cerium oxide nanoparticles. Unlike hydrothermal methods, solvothermal methods use organic solvents as the reaction solution to produce nanomaterials of various sizes and shapes under high temperatures and pressures.[49] Devaraju and coworkers presented a quick solvothermal method to prepare nanoceria. They investigated the effectivity of incubation time on the size of the nanoceria. Cerium(III) chloride heptahydrate and cerium(III) nitrate hexahydrate were used to synthesise rod-like and sphere-like cerium oxide, respectively. The results indicated that thermal treatments of nanoceria at 400 °C for 20 min in a batch reactor increased the diameter of rod-like cerium oxide to 500–1000 nm, from 10–20 nm, with 5 min of calcination. The size of sphere-like cerium oxide was also increased from 100–200 nm to 500–600 nm. Besides, their

Table 2 Synthesis of cerium oxide nanoparticles using hydrothermal methods

Precursors		Reactant		Temp.	Time (hours)	Size (nm)	Surfactant/ coating	Morphology	Valence states	Ref.
Cerium(III) nitrate hexahydrate (mol L^{-1})	0.05	Sodium hydroxide (mol L^{-1})	6	180	24	5–60	N/A	Nanocubes	Ce^{3+} & Ce^{4+}	37
	0.05		6	100	6	(7–9) × (50–200)		Nanorods		
	0.05	Ammonium hydroxide (mol L^{-1})	6	180	24	3–20		Nanocubes & nano truncated octahedra		
	0.17		0.68	180	24	6–35		Nano-octahedra		
	0.03	Trisodium phosphate (mol L^{-1})	0.0025	180	10	150–260		Submicronic octahedra		
	0.13	Sodium hydroxide (mol L^{-1})	11	90	24	30 × (25–200)	N/A	Nanorods	Ce^{3+} (24.3%)	47
			1.8	90	24	38		Nano polyhedra	Ce^{3+} (25.3%)	
			11	180	24	12.5		Nanocubes	Ce^{3+} (24.3%)	
Ammonium cerium(IV) nitrate (mol L^{-1})	0.06	Acetic acid (mol L^{-1})	2.2	220	12	5–10	Apoferritin	Nanocubes	Ce^{3+} (70%)	48

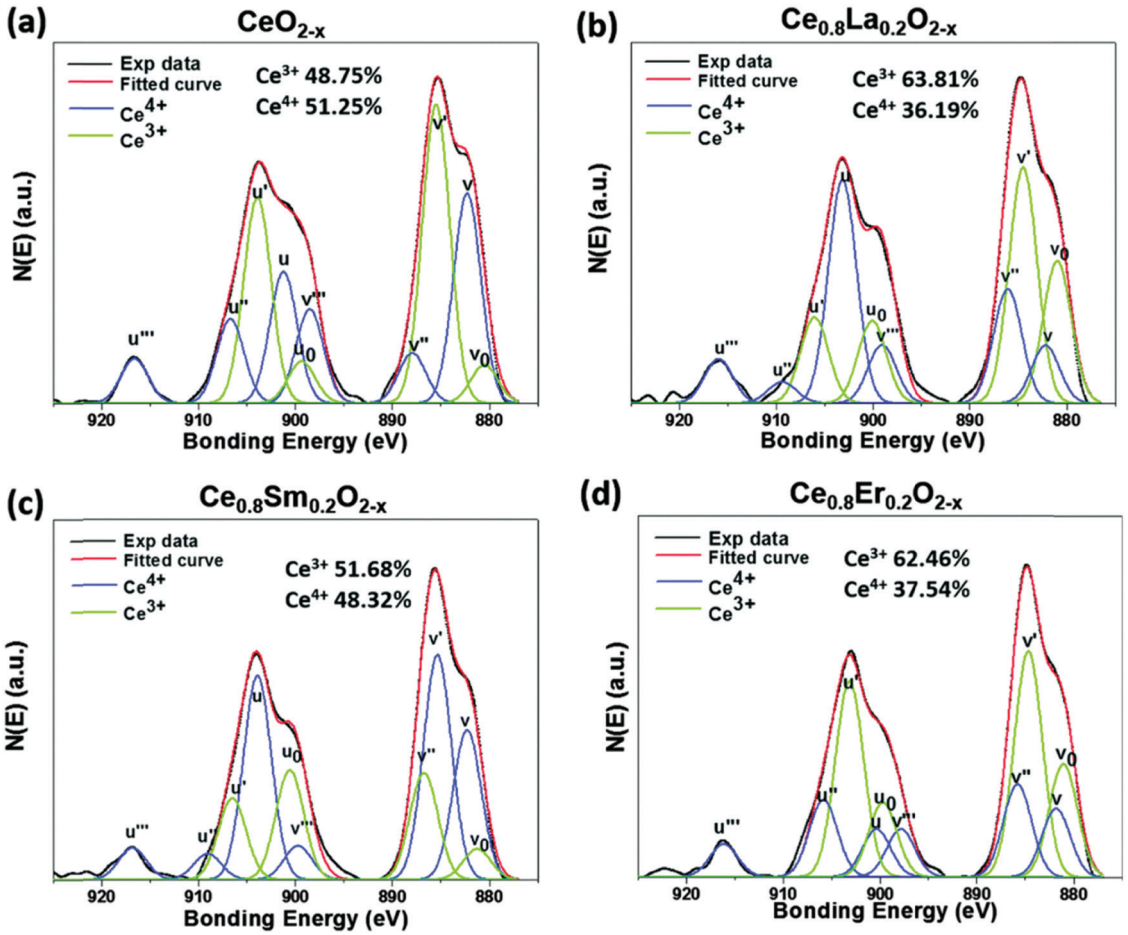

Fig. 2 XPS spectrum of Ce (3d).[46] (a) Pure dextran CNPs, (b) 20 mole% lanthanum-doped CNPs, (c) 20 mole% samarium-doped CNPs, and (d) 20 mole% erbium-doped CNPs. Reproduced from A. Gupta, S. Das, C. J. Neal and S. Seal, *J. Mater. Chem. B*, 2016, **4**, 3195–3202 with permission from The Royal Society of Chemistry.

results suggested that the particle size could be affected by the solubility of the starting materials in different organic solvents. Rod-like nanoceria prepared in ethanol solution (200–500 nm) exhibited a smaller diameter than those prepared in methanol solution (500–800 nm) (Fig. 3).[40] In a different study, Camacho-Ríos *et al.*[50] sought to synthesise nanoceria *via* a solvothermal method with the application of ethylenediaminetetraacetate acid (EDTA), citric acid and ascorbic acid as surface capping/stabilising agents. The TEM images showed that citric acid-stabilised nanoceria had the best dispersion with a particle size of around 7–9 nm and a quasi-spherical shape. Importantly, Ce^{4+} (27%) and Ce^{3+} (22%) were detected on the surface of the cerium oxide nanoparticles.

2.1.4 Microemulsification micelle methods. Table 4 summarises the microemulsification micelle methods used to synthesise cerium oxide nanoparticles. Microemulsion is a balance system including an aqueous phase, an oil phase and a surfactant. Zhang *et al.* employed the microemulsion technique to prepare nanoceria.[51] Subsequently, the resulting nanoceria were annealed at 350 °C or 600 °C for two hours. The results indicated that the increasing temperature decreased the size of the particles from 65 nm to 6 nm. Besides, the X-ray absorption spectra (XAS) showed that Ce^{4+} increased on the surface of the nanoceria when annealed at a higher temperature and changed entirely to Ce^{4+} when the annealing temperature reached 500 °C. Additionally, Sathyamurthy and coworkers prepared well-defined polyhedral nanoceria using the reverse micellar method. Their study findings showed that a narrow size distribution with an average size of 5 nm was achieved and the physicochemical properties of the nanoceria were retained by using the reverse micellar method.[52]

2.2 Green synthesis methods

Table 5 summarises the different green methods used to synthesise cerium oxide nanoparticles. High dosage of cerium oxide nanoparticles synthesised by a conventional chemical method showed cytotoxicity to many cell lines such as human bronchial epithelium cells,[53] macrophages,[54] human fibroblasts[55] and other cancer cells.[56,57] Some studies showed that ceria nanorods exhibited stronger cytotoxicity than the other shapes of nanoceria.[58,59] In a study by Forest *et al.*,[50] nanoceria with a size of around 5 to 8 nm were synthesised by hydrothermal methods. The resulting nanoceria at a concentration of 30 μg ml^{-1} increased the production of TNF-α and caused cytotoxicity to RAW264.7. Besides,

Table 3 Synthesis of cerium oxide nanoparticles using solvothermal methods

Precursors		Reactant		Temp.	Time (min)	Size (nm)	Surfactant/ coating	Morphology	Valence states	Ref.
Cerium(III) chloride heptahydrate (mol L^{-1})	0.21	Ethanol	100%	400	5	(10–20) × (50–100)	N/A	Nanorods	Ce^{3+} & Ce^{4+}	40
		Ethanol		400	10	(30–50) × (500–1000)		Nanorods		
		Ethanol		400	15	(200–500) × (1000–2000)		Nanorods		
		Ethanol		400	20	(200–500) × (1000–2000)		Nanorods		
		Ethanol		500	60	(200–500) × (1000–2000)		Nanorods		
		Methanol	100%	500	60	(500–800) × (1000–2000)		Nanorods		
Cerium(III) nitrate hexahydrate (mol L^{-1})	0.25	Ethanol	100%	400	5	100–200		Nanosphere		
		Ethanol		400	10	150–300		Nanosphere		
		Ethanol		400	15	300–500		Nanosphere		
		Ethanol		400	20	500–600		Nanosphere		
		Ethanol		500	60	300–500		Nanosphere		
		Methanol	100%	500	60	400–500		Nanosphere		
Cerium(III) nitrate hexahydrate (mol L^{-1})	0.08	Ethanol	90%	190	24	6	Citric acid	Nanosphere	Ce^{3+} (27%) & Ce^{4+} (22%)	50
				190	24	6	Ascorbic acid	Nanosphere	N/A	
				190	24	6	EDTA	Nanosphere		
				160	24	6	Citric acid	Nanosphere		
				160	24	6	Ascorbic acid	Nanosphere		
				160	24	6	EDTA	Nanosphere		

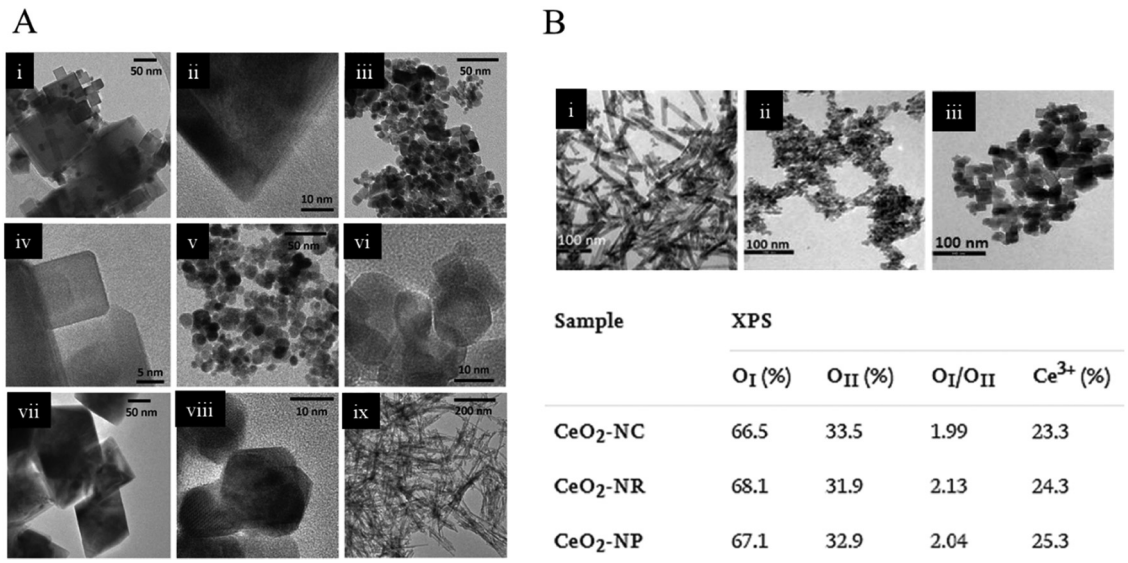

Sample	XPS			
	O_I (%)	O_{II} (%)	O_I/O_{II}	Ce^{3+} (%)
CeO_2-NC	66.5	33.5	1.99	23.3
CeO_2-NR	68.1	31.9	2.13	24.3
CeO_2-NP	67.1	32.9	2.04	25.3

Fig. 3 TEM images of cerium oxide nanoparticles synthesised by hydrothermal methods. (A) TEM and HRTEM images of the various morphologies of nanoceria synthesised by Trenque *et al.*: (i and iv) nanocubes (NCs), (vii and ii) submicronic octahedra (SOs), (v and viii) nano-octahedra (NOs), (iii and vi) mixture of nanocubes and truncated nano-octahedra (NCOs) and (ix) nanorods (NRs).[37] (B) TEM images and XPS data of the various morphologies of nanoceria synthesised by Lykaki *et al.*: (i) nanorods, (ii) nano polyhedra, and (iii) nanocubes.[47] Reproduced from I. Trenque, G. C. Magnano, M. A. Bolzinger, L. Roiban, F. Chaput, I. Pitault, S. Briançon, T. Devers, K. Masenelli-Varlot and M. Bugnet, *Phys. Chem. Chem. Phys.*, 2019, **21**, 5455–5465 with permission from The Royal Society of Chemistry.

Cheng *et al.*[60] developed nanoceria (around 20–30 nm in size) by hydrothermal methods. The resulting nanoceria displayed a significant cytotoxicity to human hepatoma SMMC-7721 cells at a concentration of 50 μg ml^{-1}. Moreover, Franchi *et al.*[55] showed that commercial nanoceria (size 25 nm) at a concentration of 10 μg ml^{-1} (Sigma-Aldrich) caused oxidative DNA damage to human fibroblasts.

To improve the biocompatibility of nanoceria at a high dosage, the green synthesis of cerium oxide nanoparticles has received extensive attention.[61] These eco-friendly bio-directed methods employed nature matrices as stabilising agents to improve the biocompatibility of nanoceria (Table 6). Many plant extracts, nutrients and fungus products have been reported to be used in the green synthesis of nanoceria.[62] In

Table 4 Synthesis of cerium oxide nanoparticles using microemulsification micelle methods

Precursors	Reactant	Temp.	Time (hours)	Size (nm)	Surfactant/coating	Morphology	Valence states	Ref.
Cerium(III) nitrate hexahydrate (mol L^{-1})	0.5 Ammonium hydroxide (mol L^{-1})	2.8 350	2	65	Cetyltrimethylammonium bromide (CTAB)	Nanosphere	Ce^{3+} & Ce^{4+}	51
		2.8 600	2	6–8				
	0.4 Sodium hydroxide (mol L^{-1})	1.7 Room temperature	1	3–5	*n*-Octane, CTAB, 1-butanol	Nano polyhedra	N/A	52

Table 5 Synthesis of cerium oxide nanoparticles using green synthesis methods

Precursors	Reactant	Surfactant/coating	Size (nm)	Morphology	Valence states	Ref.
Cerium nitrate hexahydrate	Carrageenan	Carrageenan	18–60	Mixture of spherical and cylindrical	N/A	63
Cerium nitrate hexahydrate	Extract of *Sida acuta* Brum.f. leaves	Phytoconstituents from *Sida acuta* Brum.f. and chitosan	23–90	Spherical	N/A	64
Cerium nitrate hexahydrate	Fresh egg white	Egg white	25	Spherical	N/A	65

Table 6 Advantages and disadvantages of conventional chemical synthesis methods and green synthesis methods of nanoceria

Synthesis method	Advantage	Disadvantage
Conventional chemical synthesis	• Easy to operate and scale-up • Size and shape can be tuned • Nanoceria with high crystallinity • More suitable for the preparation of small-size nanoceria	• Organic solvent residue • Energy and capital intensive • Toxic chemicals involved in the synthesis procedure
Green synthesis	• Eco-friendly • Consume much less energy • Good biocompatibility	• Mechanisms not clearly understood • Nanoceria size is variable • Lower yield

a study by Nourmohammadi *et al.*,[63] a nanoceria mixture with spherical and cylindrical particle sizes of 34 nm was synthesised *via* carrageenan hydrogelation. In this method, 50 mL of cerium nitrate (0.5 g ml^{-1}) solution was gradually added to 50 mL of carrageenan solution (20 mg ml^{-1}) and stirred vigorously for 8 h at 60 °C followed by calcination for 2 h at 600 °C. Carrageenan is a green material extracted from red seaweeds. It contains vinyl sulfonic acid groups that can help in capturing cerium ions in a solution. Cell viability studies showed that carrageenan hydrogel-capped cerium oxide nanoparticles show no toxicity to WEHI 164 cells at a concentration below 250 μg ml^{-1}. Another study investigated the antibacterial properties of chitosan-coated nanoceria synthesised from the extract of *Sida acuta* Brum.f. leaves.[64] The extract solution of *Sida acuta* Brum.f. leaves (20 mL) was dropwise added to 80 mL of cerium nitrate solution (43.3 mg ml^{-1}) and stirred for 3 h. The particles were then washed and dried for 3 h at 200 °C followed by coating with chitosan. The results showed that the spherical hybrid nanoceria (23–90 nm) could disrupt the structure of the bacterial membrane and caused the death of bacteria. However, the biocompatibility of hybrid chitosan–CeO_2 in mammalian cells has not been investigated in this study. Fresh egg white was also used as the capping agent in the green synthesis of spherical cerium oxide nanoparticles. 25 mL of fresh egg white was gently added to the equal volume of cerium nitrate (0.5 g ml^{-1}) solution. The mixture solution was stirred for 8 h at 60 °C followed by calcination for 2 h at 600 °C. The resulting nanoparticles (size 25 nm) showed excellent biocompatibility in fibroblast cells with a concentration of up to 800 μg ml^{-1}.[65]

3 Anti-ROS and anti-inflammatory properties of cerium oxide nanoparticles

The coexistence of trivalent and tetravalent cerium on the surface of nanoceria contributes to their unique regenerative anti-ROS properties and their anti-inflammation ability. Some theories of regeneration properties have been discussed in this section. Besides, *in vitro* and *in vivo* experiments also showed the anti-ROS and anti-inflammatory effects of cerium oxide nanoparticles.

3.1 Regenerative anti-ROS properties

Different studies have reported the anti-ROS and anti-inflammatory properties of cerium oxide nanoparticles.[19] Basically, the anti-ROS ability of nanoceria is related to the oxygen vacancies on its surface (Ce^{3+}/Ce^{4+} state). Trivalent cerium, as an SOD-mimetic, can react with superoxide radicals ($O_2^{\bullet -}$) to produce hydrogen peroxide ($Ce^{3+} + O_2^{-\bullet} + 2H^+ \rightarrow Ce^{4+} + H_2O_2$). In a study by Korsvik and coworkers,[10] the generation of H_2O_2 was evaluated from the nanoceria-treated $O_2^{\bullet -}$ solution. The

results showed that the nanoceria with a higher level of Ce^{3+} (40%) showed better scavenging ability of $O_2^{\bullet -}$ than that of the particles with lower Ce^{3+} (22%). In another study, Heckert *et al.* found that reducing the Ce^{3+}/Ce^{4+} ratio of nanoceria could block their SOD-mimetic activity.[66] These studies showed that the SOD-mimetic activity is mainly related to the Ce^{3+} on the surface of the nanoparticles.

In addition, like catalase (CAT), tetravalent cerium can decompose H_2O_2 to water and oxygen ($2Ce^{4+} + H_2O_2 + 2OH^- \rightarrow 2Ce^{3+} + O_2 + 2H_2O$). Pirmohamed *et al.*[67] reported that the concentration of H_2O_2 was rapidly decreased by the treatment of nanoceria with 23% of Ce^{4+} on the surface. However, no CAT mimetic activity was observed on Ce^{3+} (96%) riched nanoceria. Moreover, effective production of dissolved oxygen has been detected in H_2O_2 solution when treated with a high Ce^{4+} ratio of nanoceria. However, nanoceria with higher Ce^{3+} (96%) on the surface did not show effective production of dissolved oxygen. The results suggested that the CAT-mimetic activity of nanoceria is related to the percentage of Ce^{4+} on their particle surface. On the other hand, research showed that the H_2O_2 scavenging might also be related to Ce^{3+} on the surface of the particles ($2Ce^{3+} + H_2O_2 + 2H^+ \rightarrow 2Ce^{4+} + 2H_2O$). After being incubated with H_2O_2 solution, the results indicated that an increasing number of Ce^{4+} was present on the surface of nanoceria. In this case, the Ce^{3+} level was reduced by the oxidation of H_2O_2, which results in the increase of the Ce^{4+} level and the deoxidation of H_2O_2 to H_2O.[66]

Although the regeneration mechanism of cerium oxide has not been fully revealed, the regeneratable ROS removal mechanism of cerium oxide can still be explained by its SOD-mimetic and catalase-mimetic characteristics. First, $O_2^{\bullet -}$ or H_2O_2 has been scavenged by Ce^{3+} with the production of Ce^{4+} and H_2O_2 or H_2O. Subsequently, H_2O_2 reacts with Ce^{4+} to form O_2 and Ce^{3+}. This cycle helps in achieving the regeneration and ROS scavenging ability of nanoceria.

3.2 Pre-clinical anti-ROS and anti-inflammatory properties

Current studies also showed the anti-ROS ability of nanoceria in cells and animals. In a study by Xia *et al.*,[54] the team sought to investigate the anti-ROS ability of nanoceria in diesel exhaust particle (DEP) treated macrophages. Nanoceria of around 50 nm in size were synthesised by a hydrothermal method. 40% of the ROS level in the macrophages was quenched by the treatment of 25 μg ml^{-1} of nanoceria. In another study, Hirst *et al.*[19] indicated that 1.4 μg ml^{-1} of cerium oxide nanoparticles (5 nm) synthesised by the precipitation method could scavenge almost 100% of ROS in LPS-stimulated macrophage cells. Meanwhile, the nanoceria did not damage the macrophages up to 1.4 μg ml^{-1} of cerium oxide. *In vivo* studies showed that the administration of 500 μg kg^{-1} of cerium oxide nanoparticles reduced the malonaldehyde (MDA) level in CCl_4-induced CD1 mice. Moreover, the administration of 500 μg kg^{-1} of cerium oxide nanoparticles reduced the malonaldehyde (MDA) level in CCl_4-induced CD1 mice. In this study, nanoceria showed promising anti-ROS and anti-inflammatory abilities in LPS-stimulated macrophages without causing any damage to the cells and major organs of mice. However, the relationship between the Ce^{3+}/Ce^{4+} ratio of nanoceria and their anti-ROS and anti-inflammatory properties has not been investigated in this study.

Additionally, Gupta *et al.*[46] investigated the anti-ROS ability of nanoceria (synthesised *via* the precipitation method) in H_2O_2 treated human umbilical vein endothelial cells (HUVECs). The results indicated that higher Ce^{3+}-containing (63%) nanoceria (0.17 μg ml^{-1}) exhibited around 2-fold higher efficiency of the ROS scavenging in HUVECs than the nanoceria (0.17 μg ml^{-1}) with a lower percentage of Ce^{3+} on the surface (49%) (Fig. 5A). Nanoceria (8.5 μg ml^{-1}) showed no toxicity to HUVECs and the changing of surface valence state did not affect its biocompatibility Similarly, in a study by Liu *et al.*,[48] cerium oxide nanocubes were synthesised by a hydrothermal method and then coated with apoferritin (Aft–CeO_2). The X-ray photoelectron spectroscopy showed that Aft–CeO_2 had 70% of Ce^{3+} on the surface of the nanoceria, while the non-coated nanoceria had no Ce^{3+} on its surface. The anti-ROS study suggested that Aft–CeO_2 (4.25 μg ml^{-1}) had more than three times higher ROS scavenging efficiency than the non-coated nanoceria (4.25 μg ml^{-1}). These two studies suggest that nanoceria with a high Ce^{3+}/Ce^{4+} state could show enhanced anti-ROS ability.

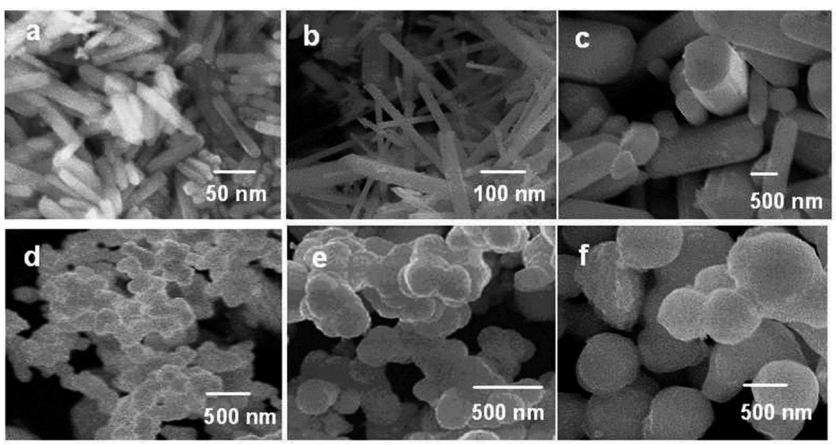

Fig. 4 Field emission scanning electron microscopy images of the as-prepared samples using $CeCl_3{\cdot}7H_2O$ (a–c) and $Ce(NO_3)_3{\cdot}6H_2O$ and (d–f) as the starting materials in ethanol at 400 °C for 5 min (a and d), 10 min (b and e), and 20 min (c and f).[40]

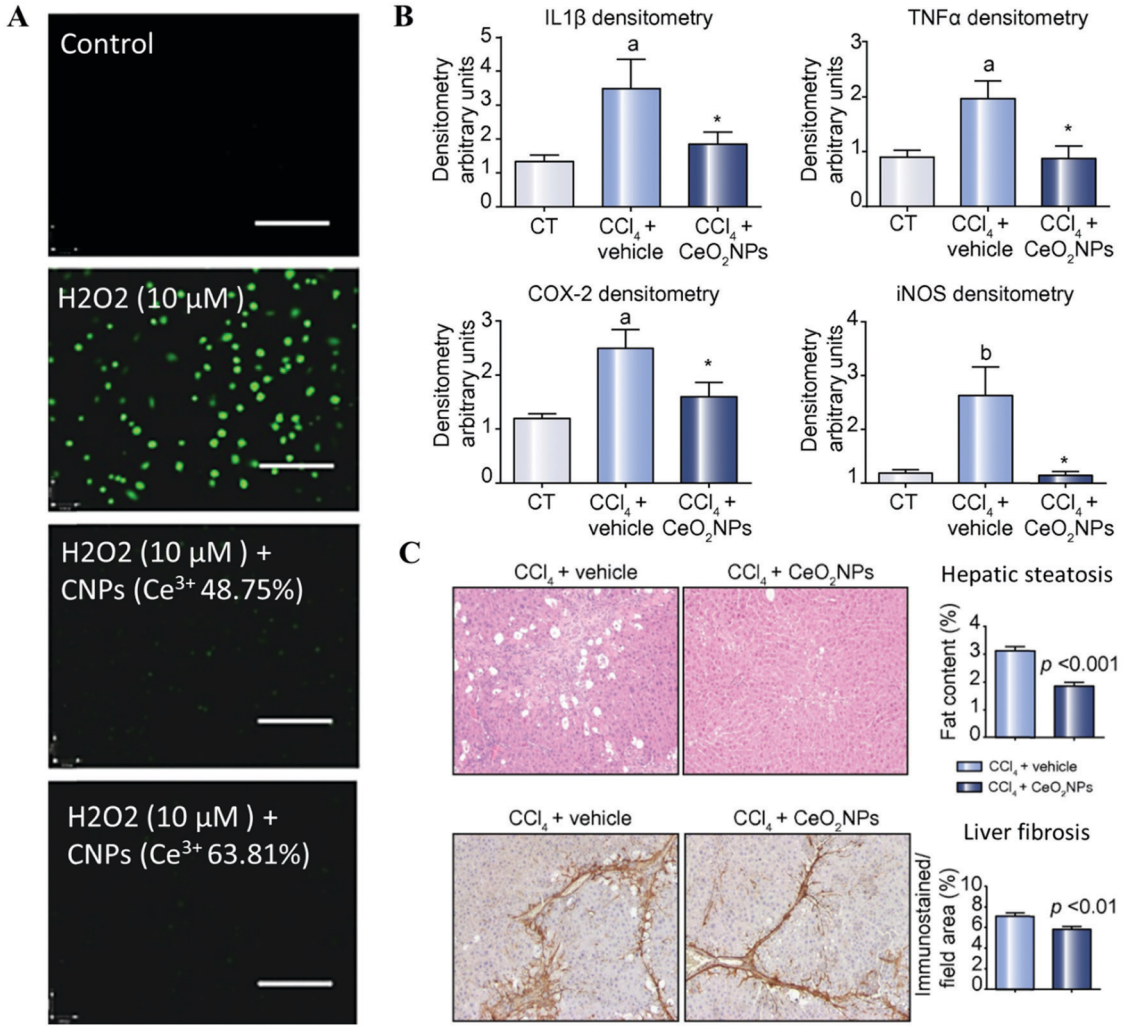

Fig. 5 Anti-ROS and anti-inflammatory capabilities of nanoceria. (A) Intracellular ROS scavenging properties of CNPs evaluated by confocal microscopy. HUVEC cells treated with 1 μM of CNPs with (Ce^{3+} 40%) or without (Ce^{3+} 64%) doping exhibited decreased intracellular ROS. 10 μM of H_2O_2 was used to stimulate the ROS level. Scale bar: 100 μm.[46] (B) Effects of CeO_2NPs on hepatic inflammation in CCl_4-treated rats. The bar charts show the densitometric analysis of all the inflammatory protein levels normalised to GAPDH. The results are given as means ± SE; (a), $p < 0.05$; (b), $p < 0.01$ *vs.* control; *$p < 0.05$ *vs.* CCl_4 + vehicle.[71] (C) Hepatic steatosis and liver fibrosis of representative liver sections obtained from CCl_4-treated rats receiving vehicle or CeO_2 NPs. The quantitative measurement is shown at the right of the figure.[71] Fig. 5A is reproduced from A. Gupta, S. Das, C. J. Neal and S. Seal, *J. Mater. Chem. B*, 2016, **4**, 3195–3202 with permission from The Royal Society of Chemistry.

In 2018, Chen *et al.*[68] synthesised nanoceria (size 285 nm) *via* the green synthesis method. The *Camellia sinensis* filtrate was mixed with ceric ammonium nitrate at 50 °C followed by calcination at 600 °C for 1 h to form the spherical nanoceria. These nanoceria were able to reduce the relative ROS level (25%) at a concentration of 100 μg ml^{-1}. ROS is a critical factor in many inflammatory responses.[69] Hence, nanoceria in the regulation of ROS in the human body may also affect the signalling pathway of some inflammatory cytokines. Chen *et al.* also investigated the anti-inflammatory properties of nanoceria in LPS-stimulated macrophages. The results indicated that nanoceria reduced the expression of COX-2 and iNOX at a concentration of 5 μg ml^{-1}. Consistently, *in vivo* studies showed that rat serum cytokines such as TNF-α, IL-1α, and IL-1β were decreased in nanoceria-treated rats. Besides, Selvaraj *et al.*[70] indicated that 8.6 μg ml^{-1} of nanoceria (purchased from the NanoScale corporation) reduced the over-expression of TNF-α, COX-2, iNOX, IL-1β and COX-2 in LPS-stimulated RAW264.7. Interestingly, nanoceria at this concentration increased the viability of LPS-treated macrophages from 60% to 80%. This may be due to the lower ROS and lower inflammatory protein levels, which caused less damage to the cells. Apart from this, the results from MTT-based viability assays showed no significant effects on the survivability of macrophages with a concentration of nanoceria of less than 17.2 μg ml^{-1}.

In their study, Oró *et al.*[71] also suggested that TNF-α, IL-1β, COX-2 and iNOS expression levels in CCl_4-induced rats can be reduced by synthesising nanoceria (0.1 mg kg^{-1}) using the precipitation method (Fig. 4). These results suggested that nanoceria from different synthesis methods have great potential to be used as therapeutic agents for ROS-related

and inflammatory diseases (Fig. 5B). In addition, the progression of hepatic steatosis and liver fibrosis was inhibited by nanoceria (Fig. 5C). Nanoceria were found to accumulate in the rat spleen, liver, lungs, and kidneys after 90 minutes of IV injection. Moreover, it is interesting that nanoceria could exist in these organs for more than eight weeks.

The studies mentioned above showed that nanoceria obtained from different synthesis methods possess promising anti-ROS and anti-inflammatory abilities in both *in vitro* and *in vivo* studies. They also showed good biocompatibility in cells and animal organs. Overall, it is suggested that nanoceria have great potential to be used as therapeutic agents for ROS-related and inflammatory diseases.

4 Conclusions and future perspectives

The anti-ROS activity and self-regeneration ability of cerium oxide nanoparticles make them excellent candidates for ROS scavengers. Besides, they are considered as alternative therapeutic agents for various chronic diseases.[72–74] Nanoceria synthesised by precipitation, hydrothermal and solvothermal methods have a controlled size and morphology. The green synthesis method provides nanoceria a better biocompatibility. Importantly, the studies indicated that more Ce^{3+} on the surface of nanoceria helps them work as SOD-mimetics, while Ce^{4+} is responsible for the CAT-mimetic activity of nanoceria. Moreover, the results suggested that higher Ce^{3+} on the surface of nanoceria could result in a better ROS scavenging efficiency of the cerium oxide nanoparticles.

The concentration of reactants and the reaction temperature affect the physical and chemical properties of cerium oxide nanoparticles. Hence, the optimisation of their synthesis methods according to the requirements of biological applications is essential. Particularly, the surface percentage of Ce^{3+} and Ce^{4+} should be evaluated and reported in future research. Heretofore, there is no detailed study on the relationship between the Ce^{3+}/Ce^{4+} ratio and the anti-ROS and anti-inflammatory properties of nanoceria *in vitro* and *in vivo*. Current studies have been very inconsistent in recording the Ce^{3+}/Ce^{4+} ratio, thus it is difficult to compare the anti-ROS and anti-inflammatory capability of cerium oxide from different synthesis methods. It is recommended to record the ratio by using the 'percentage of Ce^{3+} or Ce^{4+}'. In this way, the relationship between the synthesis methods, Ce^{3+}/Ce^{4+} ratio, and anti-ROS and anti-inflammatory abilities of nanoceria will be better studied and compared in the future. Besides, the toxicity of cerium oxide nanoparticles of different shapes, sizes and Ce^{3+}/Ce^{4+} ratios needs to be evaluated. The long-term effects of cerium oxide nanoparticles on animals also need to be explored. In addition, the *in vivo* regeneration ability of cerium oxide nanoparticles needs to be evaluated. In the future, the targeted drug-delivery approaches[75,76] of cerium oxide nanoparticles to inflammatory diseases need to be further explored. Overall, the existing research studies suggested that cerium oxide has potential for various biomedical applications in the future.

Conflicts of interest

There are no conflicts to declare.

Acknowledgements

This work is funded by the National Health and Medical Research Council (HTT: APP1037310, APP1182347, APP200 2827) and the Heart Foundation (HTT: 102761).

References

1 V. Orera, R. Merino and F. J. S. S. I. Pena, *Solid State Ionics*, 1994, **72**, 224–231.
2 J. B. Hedrick and S. P. Sinha, *J. Alloys Compd.*, 1994, **207**, 377–382.
3 C.-H. Wang and S.-S. Lin, *Appl. Catal., A*, 2004, **268**, 227–233.
4 V. K. Ivanov, A. B. Shcherbakov and A. Usatenko, *Russ. Chem. Rev.*, 2009, **78**, 855.
5 L. De Marzi, A. Monaco, J. De Lapuente, D. Ramos, M. Borras, M. Di Gioacchino, S. Santucci and A. Poma, *Int. J. Mol. Sci.*, 2013, **14**, 3065–3077.
6 Y. Ju, B. Dong, J. Yu and Y. Hou, *Nano Today*, 2019, **26**, 108–122.
7 K. Zhu, Y. Ju, J. Xu, Z. Yang, S. Gao and Y. Hou, *Acc. Chem. Res.*, 2018, **51**, 404–413.
8 S. Das, J. M. Dowding, K. E. Klump, J. F. McGinnis, W. Self and S. J. N. Seal, *Nanomedicine*, 2013, **8**, 1483–1508.
9 I. Celardo, J. Z. Pedersen, E. Traversa and L. J. N. Ghibelli, *Nanoscale*, 2011, **3**, 1411–1420.
10 C. Korsvik, S. Patil, S. Seal and W. T. Self, *Chem. Commun.*, 2007, 1056–1058.
11 V. Baldim, F. Bedioui, N. Mignet, I. Margaill and J.-F. J. N. Berret, *Nanoscale*, 2018, **10**, 6971–6980.
12 J. M. Dowding, T. Dosani, A. Kumar, S. Seal and W. T. Self, *Chem. Commun.*, 2012, **48**, 4896–4898.
13 M. Das, S. Patil, N. Bhargava, J.-F. Kang, L. M. Riedel, S. Seal and J. J. Hickman, *Biomaterials*, 2007, **28**, 1918–1925.
14 J. Kaplan, *Nature*, 1947, **159**, 673.
15 D. Harrison, K. K. Griendling, U. Landmesser, B. Hornig and H. Drexler, *Am. J. Cardiol.*, 2003, **91**, 7–11.
16 C. A. Hitchon and H. S. El-Gabalawy, *Arthritis Res. Ther.*, 2004, **6**, 1–14.
17 U. Z. Paracha, K. Fatima, M. Alqahtani, A. Chaudhary, A. Abuzenadah, G. Damanhouri and I. Qadri, *Virol. J.*, 2013, **10**, 1–9.
18 A. El-Kenawi and B. Ruffell, *Cancer Cell*, 2017, **32**, 727–729.
19 S. M. Hirst, A. S. Karakoti, R. D. Tyler, N. Sriranganathan, S. Seal and C. M. Reilly, *Small*, 2009, **5**, 2848–2856.
20 M. S. Wason, J. Colon, S. Das, S. Seal, J. Turkson, J. Zhao and C. H. Baker, *Nanomedicine*, 2013, **9**, 558–569.
21 S. M. Hirst, A. Karakoti, S. Singh, W. Self, R. Tyler, S. Seal and C. M. Reilly, *Environ. Toxicol.*, 2013, **28**, 107–118.
22 F. Charbgoo, M. B. Ahmad and M. J. Darroudi, *Int. J. Nanomed.*, 2017, **12**, 1401.

23 Y. A. Teterin, A. Y. Teterin, A. Lebedev and I. Utkin, *J. Electron Spectrosc. Relat. Phenom.*, 1998, **88**, 275–279.
24 P. Trogadas, J. Parrondo and V. Ramani, *Electrochem. Solid-State Lett.*, 2008, **11**, B113.
25 K. Chaudhury, N. Babu, A. K. Singh, S. Das, A. Kumar and S. Seal, *Nanomedicine*, 2013, **9**, 439–448.
26 A. Clark, A. P. Zhu, K. Sun and H. R. Petty, *J. Nanopart. Res.*, 2011, **13**, 5547–5555.
27 Y. Wu, R. Zhang, H. D. Tran, N. D. Kurniawan, S. S. Moonshi, A. K. Whittaker and H. T. Ta, *ACS Appl. Nano Mater.*, 2021, **4**, 3604–3618.
28 Y. Wu, Y. Yang, W. Zhao, Z. P. Xu, P. J. Little, A. K. Whittaker, R. Zhang and H. T. Ta, *J. Mater. Chem. B*, 2018, **6**, 4937–4951.
29 Y. Liu, Y. Wu, R. Zhang, J. Lam, J. C. Ng, Z. P. Xu, L. Li and H. T. Ta, *ACS Appl. Bio Mater.*, 2019, **2**, 5930–5940.
30 M. Nadeem, R. Khan, K. Afridi, A. Nadhman, S. Ullah, S. Faisal, Z. U. Mabood, C. Hano and B. H. Abbasi, *Int. J. Nanomed.*, 2020, **15**, 5951.
31 M. Nyoka, Y. E. Choonara, P. Kumar, P. P. Kondiah and V. Pillay, *Nanomaterials*, 2020, **10**, 242.
32 E. Casals, M. Zeng, M. Parra-Robert, G. Fernández-Varo, M. Morales-Ruiz, W. Jiménez, V. Puntes and G. Casals, *Small*, 2020, **16**, 1907322.
33 B. S. Inbaraj and B.-H. Chen, *Asian J. Pharm. Sci.*, 2020, **15**, 558–575.
34 Y.-H. Lin, L.-J. Shen, T.-H. Chou and Y.-H. Shih, *J. Cluster Sci.*, 2020, 1–9.
35 M. Ramachandran, R. Subadevi and M. Sivakumar, *Vacuum*, 2019, **161**, 220–224.
36 F. Corsi, F. Caputo, E. Traversa and L. Ghibelli, *Front. Radiat. Oncol.*, 2018, **8**, 309.
37 I. Trenque, G. C. Magnano, M. A. Bolzinger, L. Roiban, F. Chaput, I. Pitault, S. Briançon, T. Devers, K. Masenelli-Varlot and M. Bugnet, *Phys. Chem. Chem. Phys.*, 2019, **21**, 5455–5465.
38 M. S. Pujar, S. M. Hunagund, D. A. Barretto, V. R. Desai, S. Patil, S. K. Vootla and A. H. Sidarai, *Bull. Mater. Sci.*, 2020, **43**, 24.
39 M. L. Hancock, R. A. Yokel, M. J. Beck, J. L. Calahan, T. W. Jarrells, E. J. Munson, G. A. Olaniyan and E. A. Grulke, *Appl. Surf. Sci.*, 2021, **535**, 147681.
40 M. K. Devaraju, S. Yin and T. Sato, *ACS Appl. Mater. Interfaces*, 2009, **1**, 2694–2698.
41 B. Elahi, M. Mirzaee, M. Darroudi, K. Sadri and R. K. Oskuee, *Colloids Surf., B*, 2019, **181**, 830–836.
42 B. Richard, J.-L. Lemyre and A. M. Ritcey, *Langmuir*, 2017, **33**, 4748–4757.
43 Y.-H. Lin, L.-J. Shen, T.-H. Chou and Y.-H. Shih, *J. Cluster Sci.*, 2021, **32**, 405–413.
44 P. A. Yurova, N. Y. Tabachkova, I. A. Stenina and A. B. Yaroslavtsev, *J. Nanopart. Res.*, 2020, **22**, 1–15.
45 S.-X. Zhang, S.-F. Xue, J. Deng, M. Zhang, G. Shi and T. Zhou, *Biosens. Bioelectron.*, 2016, **85**, 457–463.
46 A. Gupta, S. Das, C. J. Neal and S. Seal, *J. Mater. Chem. B*, 2016, **4**, 3195–3202.
47 M. Lykaki, E. Pachatouridou, S. A. Carabineiro, E. Iliopoulou, C. Andriopoulou, N. Kallithrakas-Kontos, S. Boghosian and M. Konsolakis, *Appl. Catal., B*, 2018, **230**, 18–28.
48 X. Liu, W. Wei, Q. Yuan, X. Zhang, N. Li, Y. Du, G. Ma, C. Yan and D. Ma, *Chem. Commun.*, 2012, **48**, 3155–3157.
49 R. I. Walton, *Chem. Soc. Rev.*, 2002, **31**, 230–238.
50 M. Camacho-Ríos, J. Cristóbal-García, D. Lardizabal-Gutiérrez, I. Estrada-Guel, G. Herrera-Pérez, M. Piñón-Espitia and R. Martínez-Sánchez, *Ceram. Int.*, 2020, **46**, 18791–18799.
51 J. Zhang, X. Ju, Z. Wu, T. Liu, T. Hu, Y. Xie and Z. J. Zhang, *Chem. Mater.*, 2001, **13**, 4192–4197.
52 S. Sathyamurthy, K. J. Leonard, R. T. Dabestani and M. P. Paranthaman, *Nanotechnology*, 2005, **16**, 1960–1964.
53 E.-J. Park, J. Choi, Y.-K. Park and K. J. T. Park, *Toxicology*, 2008, **245**, 90–100.
54 T. Xia, M. Kovochich, M. Liong, L. Madler, B. Gilbert, H. Shi, J. I. Yeh, J. I. Zink and A. E. Nel, *ACS Nano*, 2008, **2**, 2121–2134.
55 L. P. Franchi, B. B. Manshian, T. A. de Souza, S. J. Soenen, E. Y. Matsubara, J. M. Rosolen and C. S. Takahashi, *Toxicol. In Vitro*, 2015, **29**, 1319–1331.
56 W. Lin, Y.-w. Huang, X.-D. Zhou and Y. Ma, *Int. J. Toxicol.*, 2006, **25**, 451–457.
57 M. Pešić, A. Podolski-Renić, S. Stojković, B. Matović, D. Zmejkoski, V. Kojić, G. Bogdanović, A. Pavićević, M. Mojović and A. Savić, *Chem.-Biol. Interact.*, 2015, **232**, 85–93.
58 V. Forest, L. Leclerc, J.-F. Hochepied, A. Trouvé, G. Sarry and J. J. Pourchez, *Toxicol. In Vitro*, 2017, **38**, 136–141.
59 Z. Ji, X. Wang, H. Zhang, S. Lin, H. Meng, B. Sun, S. George, T. Xia, A. E. Nel and J. I. Zink, *ACS Nano*, 2012, **6**, 5366–5380.
60 G. Cheng, W. Guo, L. Han, E. Chen, L. Kong, L. Wang, W. Ai, N. Song, H. Li and H. Chen, *Toxicol. In Vitro*, 2013, **27**, 1082–1088.
61 S. Iravani, *Green Chem.*, 2011, **13**, 2638–2650.
62 F. Charbgoo, M. B. Ahmad and M. Darroudi, *Int. J. Nanomed.*, 2017, **12**, 1401.
63 E. Nourmohammadi, R. K. Oskuee, L. Hasanzadeh, M. Mohajeri, A. Hashemzadeh, M. Rezayi and M. Darroudi, *Ceram. Int.*, 2018, **44**, 19570–19575.
64 R. Senthilkumar, V. Bhuvaneshwari, R. Ranjithkumar, S. Sathiyavimal, V. Malayaman and B. Chandarshekar, *Int. J. Biol. Macromol.*, 2017, **104**, 1746–1752.
65 H. Kargar, H. Ghazavi and M. Darroudi, *Ceram. Int.*, 2015, **41**, 4123–4128.
66 E. G. Heckert, A. S. Karakoti, S. Seal and W. T. Self, *Biomaterials*, 2008, **29**, 2705–2709.
67 T. Pirmohamed, J. M. Dowding, S. Singh, B. Wasserman, E. Heckert, A. S. Karakoti, J. E. King, S. Seal and W. T. Self, *Chem. Commun.*, 2010, **46**, 2736–2738.
68 G. Chen and Y. Xu, *Mater. Sci. Eng., C*, 2018, **83**, 148–153.
69 H. Blaser, C. Dostert, T. W. Mak and D. Brenner, *Trends Cell Biol.*, 2016, **26**, 249–261.

70 V. Selvaraj, N. D. Manne, R. Arvapalli, K. M. Rice, G. Nandyala, E. Fankenhanel and E. R. Blough, *Nanomedicine*, 2015, **10**, 1275–1288.
71 D. Oró, T. Yudina, G. Fernández-Varo, E. Casals, V. Reichenbach, G. Casals, B. G. de la Presa, S. Sandalinas, S. Carvajal and V. Puntes, *J. Hepatol.*, 2016, **64**, 691–698.
72 S. V. Kyosseva, L. Chen, S. Seal and J. F. McGinnis, *Exp. Eye Res.*, 2013, **116**, 63–74.
73 V. Selvaraj, N. D. Manne, R. Arvapalli, K. M. Rice, G. Nandyala, E. Fankenhanel and E. R. Blough, *Nanomedicine*, 2015, **10**, 1275–1288.
74 J. Niu, A. Azfer, L. M. Rogers, X. Wang and P. E. Kolattukudy, *Cardiovasc. Res.*, 2007, **73**, 549–559.
75 W. He, N. Kapate, C. W. Shields IV and S. Mitragotri, *Adv. Drug Delivery Rev.*, 2020, **165**, 15–40.
76 W. Ulbrich and A. Lamprecht, *J. R. Soc., Interface*, 2010, **7**, S55–S66.